# Quantificational and Statistical Analysis of the Differences in Centrosomal Features of Untreated Lung Cancer Cells and Normal Cells

**Dansheng Song,** M.S.,  **Inna Fedorenko,** B.A.,  **Marianna Pensky,** Ph.D.,
**Wei Qian,** Ph.D.,  **Melvyn S. Tockman,** M.D., Ph.D.,  and
**Tatyana A. Zhukov,** Ph.D., P.M.I.A.C.

OBJECTIVE: To distinguish untreated lung cancer cells from normal cells through quantitative analysis and statistical inference of centrosomal features extracted from cell images.
STUDY DESIGN: Recent research indicates that human cancer cell development is accompanied by centrosomal abnormalities. For quantitative analysis of centrosome abnormalities, high-resolution images of normal and untreated cancer lung cells were acquired. After the images were preprocessed and segmented, 11 features were extracted. Correlations among the features were calculated to remove redundant features. Ten nonredundant features were selected for further analysis. The mean values of 10 centrosome features were compared between cancer and normal cells by the two-sample t-test; distributions of the 10 features of cancer and normal centrosomes were compared by the two-sample Kolmogorov-Smirnov test.
RESULTS: Both tests reject the null hypothesis; the means and distributions of features coincide for normal and cancer cells. The 10 centrosome features separate normal from cancer cells at the 5% significance level and show strong evidence that all 10 features exhibit major differences between normal and cancer cells.
CONCLUSION: Centrosomes from untreated cancer and normal bronchial epithelial cells can be distinguished through objective measurement and quantitative analysis, suggesting a new approach for lung cancer detection, early diagnosis and prognosis. (Anal Quant Cytol Histol 2010;32:280–290)

**Keywords:** centrosome, Kolmogorov-Smirnov test, lung cancer, statistical analysis, t-test.

The centrosome is a cellular organelle that functions as the microtubule organizing center of interphase and mitotic cells.[1] The centrosome duplicates itself only once during each cell cycle with duplication beginning near the G1-S transition and completing during the G2 phase. Duplicated centrosomes separate to produce two mitotic spindle poles that organize the mitotic apparatus. Centrosomes play critical roles in processes that ensure proper segregation of chromosomes and maintain the genetic stability of human cells.[2,3] Centrosomal abnormalities are detected in various types of human cancers, such as cancers of the lung, breast, gallbladder, bone, pancreas, colon, rectum, head, neck, prostate, and ovaries.[4,5] Recent evidence indicates that loss of centrosomal integrity may be a major cause of genetic instability underlying various human cancers.[3-7] Aneuploidy of non–small cell lung cancer is associated with centrosomal abnormalities.[8] In the lung, important findings suggest that centrosomal abnormalities may develop at a relatively early stage of lung carcinogenesis. Moreover, it was shown that stepwise progression of centrosome defects is associated with local lung tumor progression to a more advanced stage and with accelerating the metastatic process of lung carcinoma cells.[9]

This article provides for the first time, an objective, quantitative assessment of centrosomal abnormalities. This quantitative centrosomal assessment demonstrates that untreated lung cancer cells can be successfully distinguished from normal lung cells and identifies a new approach for lung cancer detection, early diagnosis, and prognosis.

## Materials and Methods
### Image Acquisition

Centrosomal images were acquired in the Analytic Microscopy Core at the H. Lee Moffitt Cancer Center. A549 lung cancer cells and BEAS 2B normal bronchial epithelial cells were grown in RPMI (Invitrogen, Carlsbad, California, U.S.A.) with 10% fetal bovine serum (Invitrogen) and bronchial epithelial growth medium (BEGM) (Lonza Walkersville Inc., Walkersville, Maryland, U.S.A.) supplemented with a BEGM bullet kit, respectively. Cells were plated and grown on coverslips in a 6-well plate at 37°C with 5% $CO_2$. Cells were fixed using 4% paraformaldehyde solution for 30 minutes at 4°C and permeabilized using 0.5% Triton X solution (Sigma-Aldrich, St. Louis, Missouri, U.S.A.). Following blocking with 2% bovine serum albumin, cells were stained with γ-Tubulin anti-body (Sigma-Aldrich). Cells were then incubated with AlexaFluor 594 secondary antibody (Invitrogen) and mounted using ProLong Antifade with DAPI (Invitrogen). A DMI6000 inverted Leica TCS AOBS SP5 tandem-scanning confocal microscope (Leica Microsystems GmbH, Wetzlar, Germany) was used to image the cells, under a ×100 oil immersion objective with scanning speed of 100 Hz per each 2048×2048 frame (Figure 1a and b). The LAS AF software suite (Leica Microsystems GmbH) was used to image the cells and compile the maximum projections from Z-stacks. The acquired image has a resolution of 75.7 nm.

### Selection of Region of Interest

Regions of interest (ROIs) are selected to include one cell with at least one centrosome (Figure 1c and d).

### Preprocessing

Although some centrosomal shape features are preserved at 75.7-nm resolution, for reliable segmentation, feature extraction, and analysis, further resolution enhancement is needed. Lagrange interpolation polynomials can be used for this task.[10]

Two-dimensional first-degree Lagrange polynomial interpolation is implemented to enhance resolution of the images. This is a linear interpolation technique that, at any point, uses information given only by the two adjacent pixels and leads to a good approximation of image boundaries. Linear interpolation is performed first in one direction and then in the other. For example, to obtain interpolation at point P, one needs to interpolate at points $R_1$ and $R_2$ using information from $Q_{11}$, $Q_{21}$, and $Q_{12}$, $Q_{22}$, respectively. After that, interpolation at the point P is obtained using the formulae below.
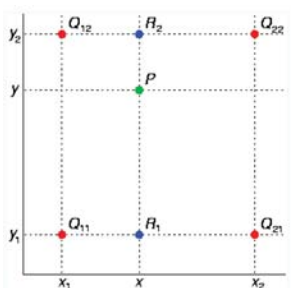


$$f(R_1) = \frac{x_2 - x}{x_2 - x_1}f(Q_{11}) + \frac{x - x_1}{x_2 - x_1}f(Q_{21})$$

$$f(R_2) = \frac{x_2 - x}{x_2 - x_1}f(Q_{12}) + \frac{x - x_1}{x_2 - x_1}f(Q_{22})$$

$$f(P) = \frac{y_2 - y}{y_2 - y_1}f(R_1) + \frac{y - y_1}{y_2 - y_1}f(R_2)$$

This procedure provides the resolution enhancement necessary for successful feature extraction and measurement (Figure 2).
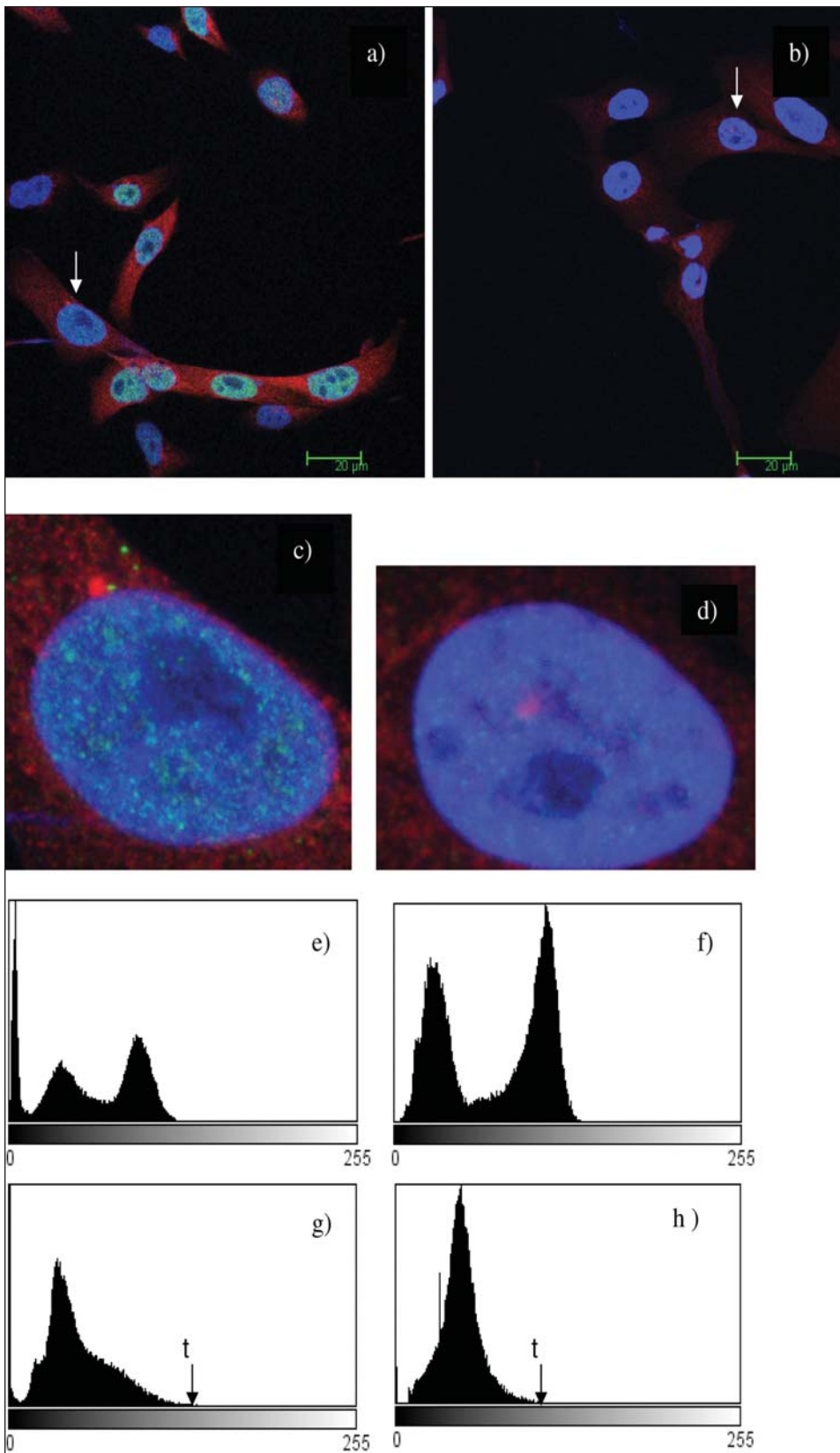
**Figure 1**   (a and b) Original images under ×100 oil-immersion objective, for a total magnification of ×1,000. (c and d) Full-color centrosome region of interest images taken from (a) and (b), respectively. (e and f) are histograms of (c) and (d). (g and h) are the red channel histograms of (c) and (d). t = optimized thresholds.
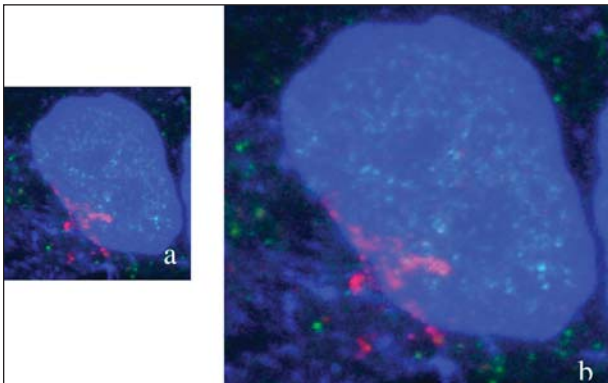
**Figure 2**   (a) A color RGB image taken from untreated cancer cell image, which includes centrosomes belonging to this cell. (b) Interpolated image of (a). Its size is twice that of image (a). To balance the image processing time and resolution of the image, two times interpolation is chosen.

*Image Segmentation*

Before extracting centrosomal features, the centrosomes need to be isolated from other parts of the cells in images (Figure 3). After comparing various thresholding methods, Kapur's maximum entropy-based thresholding[11] was selected and implemented for this task because of the consistency and accuracy of its outputs. The method considers the foreground (centrosomes) and the background (other parts of the cells) of an image as two different signal sources and finds the threshold that maximizes the sum of the entropies of the two classes as follows.

Let an image have $N$ pixels with gray level ranging from 0 to $L$-1. Denote by $h(i)$, the number of occurrences of gray level $i$, and by $P_i = h(i)/N$, the probability of occurrences of gray level $i$. The method finds threshold $t$, which maximizes

$$f(t) = H(0, t) + H(t, L)$$

where   $H(0,t) = -\sum_{i=0}^{t-1} \frac{P_i}{w_0} \ln \frac{P_i}{w_0}, \quad w_0 = \sum_{i=0}^{t-1} P_i$ ,

$H(t,L) = -\sum_{i=t}^{L-1} \frac{P_i}{w_1} \ln \frac{P_i}{w_1}, \quad w_1 = \sum_{i=t}^{L-1} P_i$ .

The entropy segmentation threshold affected by the pixel number of the centrosome space ($P_i = h(i)/N$,), and depends on the number of channels. From Figure 1e and f, we can find different distributions of pixel values (histograms) of these two color images. The entropy threshold did not work well on these color images. We chose not to apply entropy threshold on full-color image; instead, we applied the entropy threshold on only the red channel because all centrosomal information can be found in this channel. Figure 1g and h show the red channel histograms of the two ROIs images. They have similar distributions with one peak. In fact, all of the red channel histograms of centrosome ROI images have similar monotonic distributions. After the optimization procedure, all of the thresholds stopped on the right feet of the peaks. We got consistently accurate thresholds.

*Feature Extraction*

After centrosomes are isolated, 11 specific centrosomal features are extracted, to be later used for discrimination between cancer cells and normal cells. The definitions of these 11 features include:

(1) Number: Number of centrosomes per cell.
(2) Area: The number of pixels in the area of a centrosome.
(3) Fragment: Defected centrosomes may fragment into multiple microtubule organizing centers.[5]

$F = \begin{cases} 1 & \text{if there is fragment in a centrosome.} \\ 0 & \text{if there is no fragment in a centrosome.} \end{cases}$

(4) Area/Box: The ratio between the numbers of pixels in the area of a centrosome and the area of its bounding box. It is always ≤1.
(5) Aspect: The ratio between the major axis and the minor axis of the ellipse, which is equivalent to a centrosome (has the same area as the centrosome). Aspect is always ≥1.
(6) Mean diameter: An average length of the diameters that are drawn through the centrosomal centroid at 2-degree increments.
(7) Perimeter ratio: The ratio between the convex perimeter of a centrosome and its actual perimeter. Perimeter ratio is always ≤1.
(8) Roundness: Roundness is equal to the squared perimeter of a centrosome divided by 4πA, where A is the area of the centrosome. Roundness demonstrates how far the shape of the centrosome deviates from a circle. The larger the roundness parameter, the further the deviation of the shape from being round. If a centrosome has a circular shape, its roundness = 1, otherwise, it is >1.
(9) Fractal dimension[12]: The fractal dimension is a measurement of roughness. The rougher
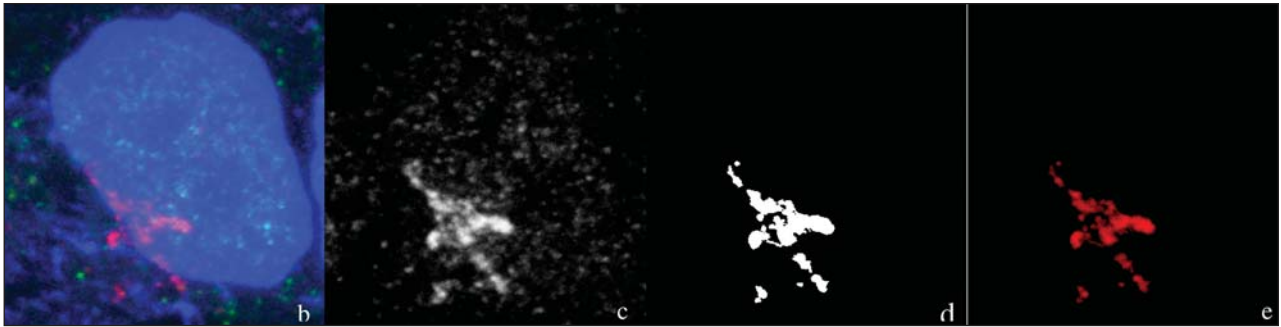
**Figure 3**   (b) Interpolated image. (c) The red channel of RGB image b. This channel shows the signal from the 594 laser reading the Alexa Fluor 594 secondary antibody bound to γ-Tubulin. All of the centrosome's information can be found in this channel. (d) The segmented image of image (c). This binary image will be used as the mask for separating centrosomes from the background. (e) Centrosomes are isolated from other parts of the image. It is operated on red channel. It is ready for feature extraction.

the curve, the larger is the fractal dimension. The general expression of fractal dimension is

$$FD = \lim_{S \to 0} \frac{d(\log(N))}{d(\log(1/S))}$$

where **N** is the number of hypercubes (e.g., square) of side length **S** required to cover the object (e.g., a curve).

In practice, the box counting dimension can be estimated by selecting two sets of [log(N), log(1/S)] coordinates at small value of S. An estimate of FD is then given by,

$$FD = \frac{\log(N_2) - \log(N_1)}{\log(1/S_2) - \log(1/S_1)} = \frac{\log \dfrac{N_2}{N_1}}{\log \dfrac{S_1}{S_2}}$$

(10) Intensity: An average gray level intensity in a centrosomal area is obtained by adding pixel values over the centrosomal area and then dividing by the area of the centrosome.
(11) Intensity standard deviation: The standard deviation of the gray level intensity in the centrosomal area.

*Elimination of Redundant Features*

In general, one does not need to keep redundant features (i.e., those strongly related to other features). If we adopt the correlation between the two variables as the measure of redundancy, we conclude that a feature is useful if it is not highly correlated to any of the other features.[13]

*The Two Sample* t*-Test*

After centrosome features are selected, the two sample *t*-test is performed to verify whether the two samples can be distinguished by these features. The test is carried out under the assumption that the two samples are independent and normally distributed with equal means under the null hypothesis and different means under the alternative hypothesis.

The test result h = 1 indicates rejection of the null hypothesis at α = 5% significance (95% confidence) level; h = 0 indicates failure to reject the null hypothesis. The test returns the p value p of the test and the CI (confidence interval), for the difference of means of the two samples. Although for small sample sizes, centrosome features are not necessarily normally distributed, the central limit theorem guarantees that the sample mean is normally distributed, as long as the sample size is big enough (N ≥ 30). The sample size N = 57, and 606 in our study satisfies the requirement. Therefore the two-sample *t*-test is applicable to our data.[14]

*The Two-Sample Kolmogorov-Smirnov Test*

The Kolmogorov-Smirnov (KS) test is usually used to determine whether the two samples are drawn from the same distribution (the null hypothesis) or different distributions (the alternative hypothesis). The two-sample KS test is one of the most useful and general nonparametric methods for comparing two samples, because it is sensitive to differences in both location and shape of the empirical cumulative distribution functions (CDFs) of the two samples. The KS test also has an advantage of making no assumption about the normal distribution of data.

**Table I**   *Correlations Between Shape Features of Normal Cell Centrosomes*

| | Area | Aspect | Area/box | Mean diameter | Roundness | Intensity | Perimeter ratio | Fractal dimension | Intensity SD |
|---|---|---|---|---|---|---|---|---|---|
| Area | 1.000 | −0.005 | −0.319 | 0.985 | 0.496 | 0.067 | −0.304 | 0.370 | 0.283 |
| Aspect | −0.005 | 1.000 | −0.497 | 0.074 | 0.514 | −0.261 | −0.294 | 0.246 | −0.257 |
| Area/box | −0.319 | −0.497 | 1.000 | −0.384 | −0.716 | 0.147 | 0.621 | −0.455 | 0.118 |
| Mean diameter | 0.985 | 0.074 | −0.384 | 1.000 | 0.533 | 0.041 | −0.342 | 0.367 | 0.260 |
| Roundness | 0.496 | 0.514 | −0.716 | 0.533 | 1.000 | −0.126 | −0.695 | 0.750 | −0.068 |
| Intensity | 0.067 | −0.261 | 0.147 | 0.041 | −0.126 | 1.000 | 0.253 | −0.147 | 0.732 |
| Perimeter ratio | −0.304 | −0.294 | 0.621 | −0.342 | −0.695 | 0.253 | 1.000 | −0.546 | 0.242 |
| Fractal dimension | 0.370 | 0.246 | −0.455 | 0.367 | 0.750 | −0.147 | −0.546 | 1.000 | −0.227 |
| Intensity SD | 0.283 | −0.257 | 0.118 | 0.260 | −0.068 | 0.732 | 0.242 | −0.227 | 1.000 |

The test result h = 1 means rejection of the null hypothesis that distributions of the two samples are the same at $\alpha = 5\%$ significance (95% confidence) level; the value h = 0 indicates failure to reject this hypothesis. The test also returns the p value p, and the value of the test statistic k, which quantifies the difference between distributions of the two samples and can be written as

$$k = \text{Max}(\,|\,F_1(x) - F_2(x)\,|\,)$$

where $F_1(x)$ and $F_2(x)$ are empirical CDFs of samples 1 and 2, respectively.[15]

### *Results*

After image acquisition, in total, 606 centrosomes were selected from untreated cancer cells and 57 centrosomes were selected from normal cells. The correlations among centrosomal shape features were calculated to determine feature redundancy. The number/cell and fragment features are different in nature, and different from other features; therefore we preserved number/cell and fragment as independent features. Because of this, we did not calculate correlations between these two features or between these two features and the other nine features.

Correlations between the other nine shape features for both the normal cells and untreated cancer cells results are presented in Tables I and II.

Tables I and II show that centrosome features "Area" and "Mean diameter" are highly correlated for both normal and untreated cancer cells (correlation coefficient = 0.985 and 0.938, respectively), and therefore one of these features is redundant. "Area" is the only feature that describes centrosome size, and "Mean diameter" is one of six features that describe centrosome shape. Hence, we have removed "Mean diameter" from further investigation. After "Mean diameter" is removed, the remaining 10 features are entered into the statistical analysis.

The two-sample *t*-test comparison between normal and untreated cancer centrosomes returned p values < 0.001 for all 10 features. Correspondingly, the 99.9% confidences on the mean differences of all 10 features do not contain zero. This statistical result rejects the null hypothesis (i.e., h = 1 for all 10 features) (Table III). Based on the statistical test re-

**Table II**   *Correlation Between Features of Untreated Cancer Cell Centrosomes*

| | Area | Aspect | Area/box | Mean diameter | Roundness | Intensity | Perimeter ratio | Fractal dimension | Intensity SD |
|---|---|---|---|---|---|---|---|---|---|
| Area | 1.000 | 0.141 | −0.361 | 0.938 | 0.713 | 0.293 | −0.387 | 0.406 | 0.412 |
| Aspect | 0.141 | 1.000 | −0.601 | 0.241 | 0.467 | −0.192 | −0.176 | 0.176 | −0.234 |
| Area/box | −0.361 | −0.601 | 1.000 | −0.435 | −0.714 | 0.229 | 0.564 | −0.569 | 0.235 |
| Mean diameter | 0.938 | 0.241 | −0.435 | 1.000 | 0.698 | 0.347 | -0.423 | 0.377 | 0.477 |
| Roundness | 0.713 | 0.467 | −0.714 | 0.698 | 1.000 | −0.099 | −0.673 | 0.729 | −0.051 |
| Intensity | 0.293 | −0.192 | 0.229 | 0.347 | −0.099 | 1.000 | 0.132 | −0.220 | 0.699 |
| Perimeter ratio | −0.387 | −0.176 | 0.564 | −0.423 | −0.673 | 0.132 | 1.000 | −0.744 | 0.138 |
| Fractal dimension | 0.406 | 0.176 | −0.569 | 0.377 | 0.729 | −0.220 | −0.744 | 1.000 | −0.210 |
| Intensity SD | 0.412 | −0.234 | 0.235 | 0.477 | −0.051 | 0.699 | 0.138 | −0.210 | 1.000 |

**Table III**    *Two-Sample t-Test Result for Normal and Untreated Cancer Cells*

|     | No./cell | Fragment | Area | Aspect | Area/box | Roundness | Perimeter ratio | Fractal dimension | Intensity | Intensity SD |
|-----|----------|----------|------|--------|----------|-----------|-----------------|-------------------|-----------|--------------|
| h   | 1        | 1        | 1    | 1      | 1        | 1         | 1               | 1                 | 1         | 1            |
| p   | 0.000    | 0.000    | 0.622| 0.001  | 0.000    | 0.206     | 0.396           | 0.000             | 0.000     | 0.001        |
|     | e-003    | e-003    | e-003| e-003  | e-003    | e-003     | e-003           | e-003             | e-003     | e-003        |
| ci  | −3.986   | −0.719   | 86.693| −0.681| 0.054    | −0.786    | 0.011           | −0.046            | 26.536    | −3.888       |
|     | −2.337   | −0.461   | 317.54| −0.294| 0.117    | −0.244    | 0.039           | −0.021            | 41.295    | −1.700       |

sult, we can say with 99.9% confidence that for all 10 features there are significant mean differences between normal and untreated cancer centrosomes.

The difference in the distributions of centrosomal features for normal and untreated cancer cells can be also seen from the box plots below. We present box plots for five centrosomal features—centrosomal number, size, fragment, intensity, and shape. From Figure 4 we can see that these five features have different medians and, overall, different distributions. The other five box plots show a similar pattern.

The two-sample KS test confirmed the box plot results and are consistent with the two-sample *t*-test (Table IV). The test verifies that all 10 centrosome features have different distributions for the normal and untreated cancer cells (h = 1). The largest p value is 0.00015, which means that with 99.985% confidence we can claim that distribution of every feature is different for two types of cells. The test also returns the values of statistic k that indicates whether the distances between CDFs are sufficiently large to be distinct. The smallest value of k is 29.5%, which indicates that the distances between CDFs of the centrosome features for normal and untreated cancer cells are large enough to distinguish them.

We illustrate the CDF plots of five centrosomal features (Figure 5)—centrosomal number, size, fragment, intensity, and shape. One can see substantial differences between the shapes and positions of the CDF curves for centrosomal features of
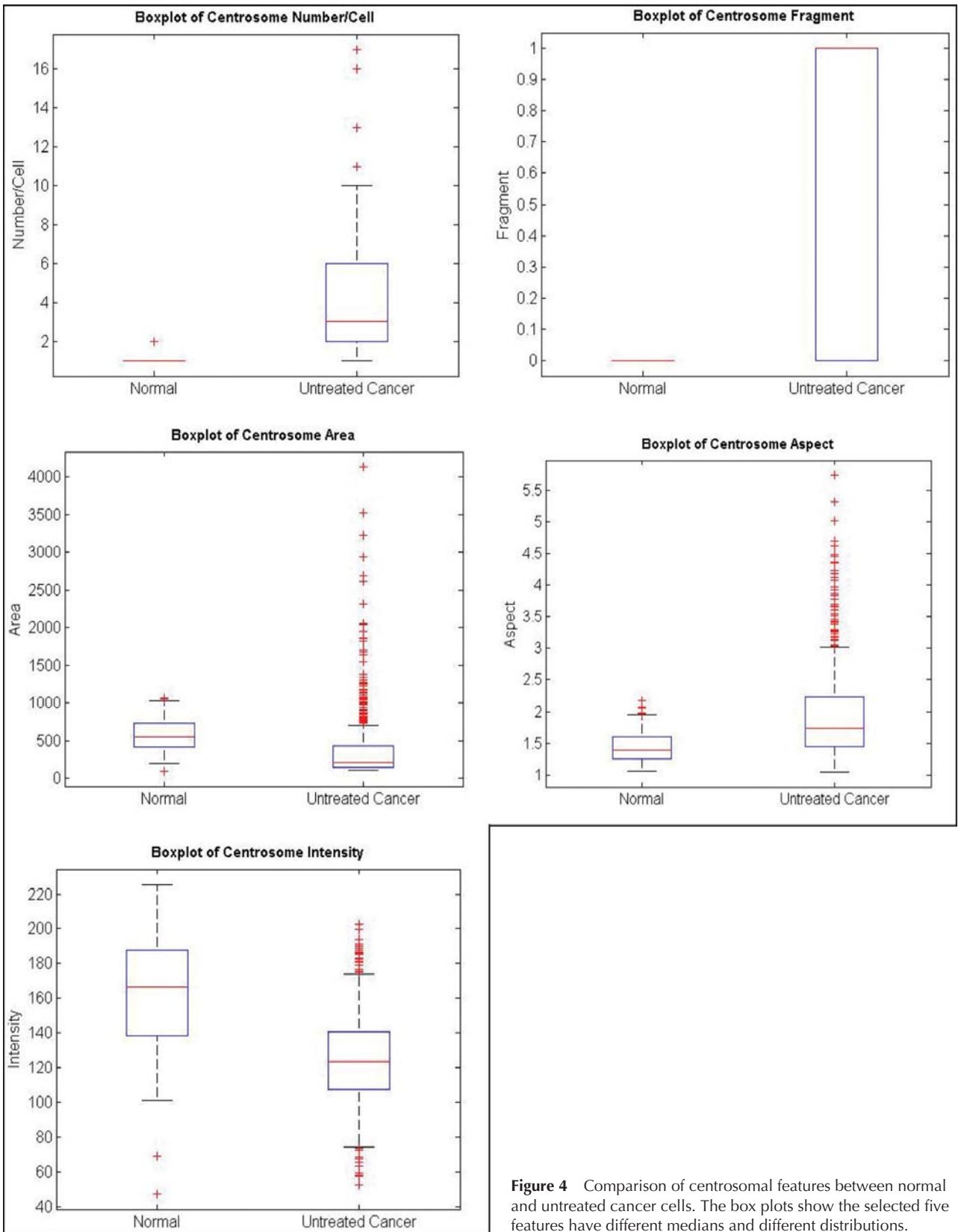
normal and untreated cancer cells. It is also apparent that the maximum distances (k) between pairs of curve are quite large. This means that all pairs of samples have different distributions and came from different populations. The remaining five CDF curves show a similar pattern.

### Discussion

Recent studies implicate centrosomal abnormalities in the pathogenesis of cancer.[16-19] However, rigorous, objective quantitation of centrosomal abnormalities has not been possible until now. The present report describes an objective procedure for characterizing and quantifying centrosomal defects that are found in lung cancer cells, but are not found in immortalized normalized bronchial epithelial cells. The term 'centrosome amplification' is commonly used to signify centrosomes that subjectively appear significantly larger than normal (as defined by the specific staining of structural centrosome components in excess of that seen in the corresponding normal tissue or cell type); supernumerary centrioles (>4) in centrosomes; inverted polarity of centrosome location; and/or >2 centrosomes are present within a cell. Amplified centrosomes also show protein hyperphosphorylation and altered functional properties, such as an increased microtubule nucleating capacity.[20-22] These structural centrosome abnormalities have been implicated as a potential cause of loss of cell and tissue architecture seen in cancer (i.e., anaplasia) through altered centrosome function and resulting in chro-

**Table IV**    *Two-Sample KS Test for Normal and Untreated Cancer Cells*

|     | No./cell | Fragment | Area | Aspect | Area/box | Roundness | Perimeter ratio | Fractal dimension | Intensity | Intensity SD |
|-----|----------|----------|------|--------|----------|-----------|-----------------|-------------------|-----------|--------------|
| h   | 1        | 1        | 1    | 1      | 1        | 1         | 1               | 1                 | 1         | 1            |
| p   | 4.976    | 2.547    | 3.626| 8.107  | 2.789    | 1.052     | 1.597           | 2.213             | 1.046     | 1.662        |
|     | e-024    | e-013    | e-016| e-008  | e-008    | e-006     | e-004           | e-008             | e-012     | e-005        |
| k   | 0.803    | 0.590    | 0.579| 0.397  | 0.409    | 0.366     | 0.295           | 0.412             | 0.511     | 0.329        |

**Figure 4**    Comparison of centrosomal features between normal and untreated cancer cells. The box plots show the selected five features have different medians and different distributions.
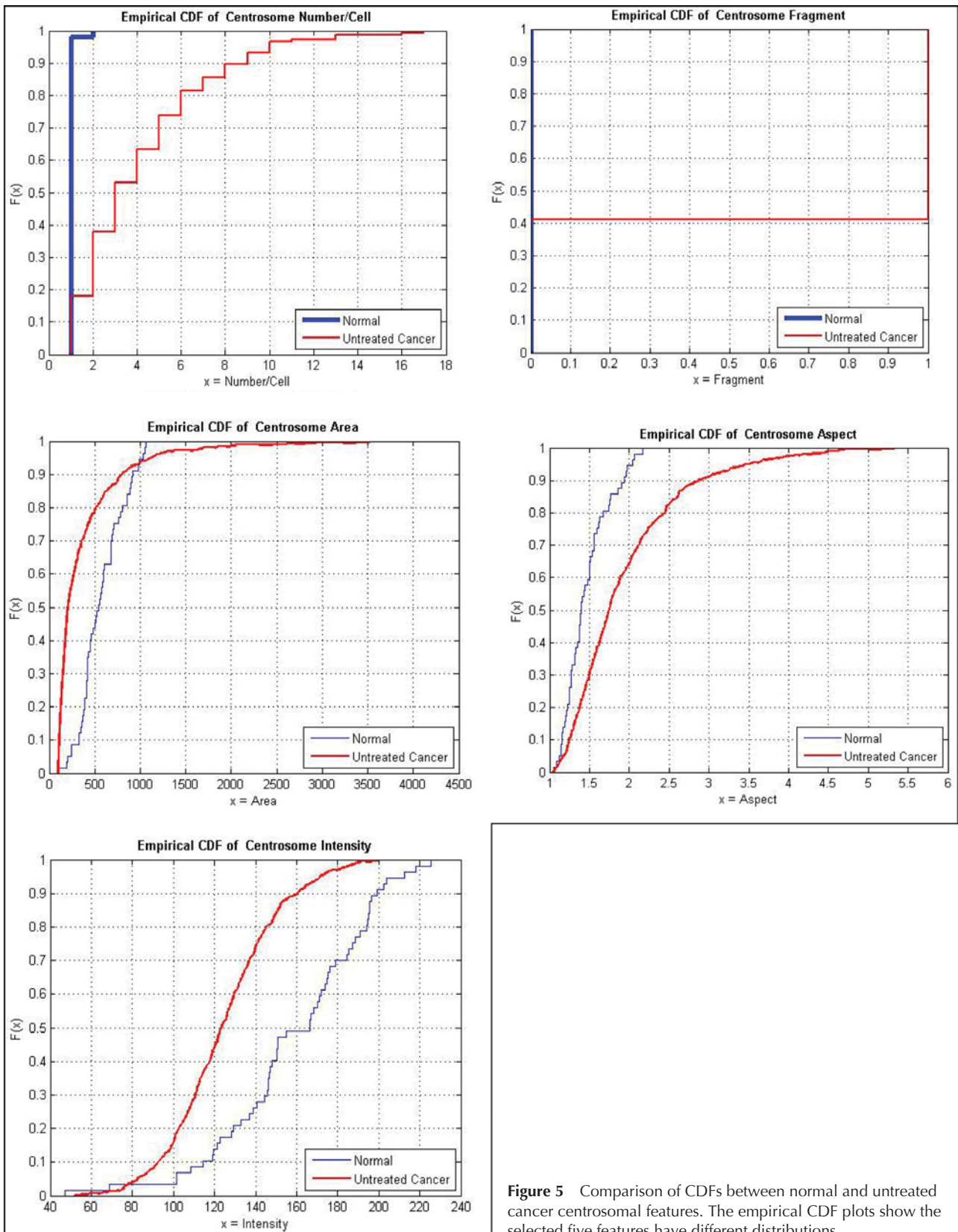
**Figure 5** Comparison of CDFs between normal and untreated cancer centrosomal features. The empirical CDF plots show the selected five features have different distributions.

mosome missegregation during mitosis as a consequence of multipolar spindle formation.[23] Data in the literature suggest that centrosomal abnormalities might be a useful marker in monitoring cancer progression.[24-27] Objective measurement, quantitative calculation and analysis of centrosomal features makes centrosomal monitoring feasible as a marker of cancer progression.

Until now, researchers commonly detect the centrosome defects through microscopy. Guo et al[28] have done limited image analysis of centrosomal features, which includes numerical and structural centrosome amplification. The cell was considered to have structural centrosome amplification if the diameter of its centrosome was greater than twice the diameter of the normal centrosome and/or if the shape of its centrosome became irregular. These investigators applied semiquantitative image analysis of cells. Other approaches for quantitation of centrosome abnormalities have used semiquantitative microscopy-based procedures that practically cannot avoid subjective judgment even with highly experienced microscopists.

Our novel quantitative analysis and statistical inference of centrosomal features, extracted from cell images avoids those pitfalls and provides objective judgment of centrosome features. The proposed method includes quantitative measurement of a centrosome features profile, capable not only of detecting feature differences but also of showing the magnitude of these differences. The diameter is not sufficient to characterize the structure or shape of a centrosome. Five features have been used in our research to describe the centrosome shape representing noncorrelated aspects of centrosome morphology. Corresponding statistical analysis of centrosome features show the significant differences of quantitatively measured features between normal and untreated cancer centrosomes. Therefore it is feasible to distinguish untreated cancer cells from normal cells through quantitative analysis of centrosomal features. Work presented in this manuscript is still in development to optimize the classification procedure to distinguish malignant from normal lung cells, independent of staining technique. We consider further studies in application of this methodology in analysis and diagnosis of clinical lung tissue specimens extremely important. Building on evidence that centrosomal abnormalities cause chromosomal instability, rather than result from late-stage tumorigenesis,[1-4,8,9] the development of an objective centrosomal measurement procedure may facilitate early detection, diagnosis, and improved prognosis.

## References

1. Nigg EA: Centrosome aberrations: Cause or consequence of cancer progression? Nature Rev Cancer 2002;2:815–825

2. Shinmura K, Iwaizumi M, Igarashi H, Nagura K, Yamada H, Suzuki M, Fukasawa K, Sugimura H: Induction of centrosome amplification and chromosome instability in p53-deficient lung cancer cells exposed to benzo[a]pyrene diol epoxide (B[a]PDE). J Pathol 2008;216:365–374

3. Fukasawa K: Oncogenes and tumour suppressors take on centrosomes. Nat Rev Cancer 2007;7:911–924

4. Bourke E, Dodson H, Andreas Merdes A, Cuffe L, Zachos G, Walker M, Gillespie D, Morrison CG: DNA damage induces Chk1-dependent centrosome amplification. EMBO Rep 2007;8:603–609

5. Saunders W: Centrosomal amplification and spindle multipolarity in cancer cells (review). Semin Cancer Biol 2005;15:25–32

6. Lentini L, Amato A, Schillaci T, Di Leonardo A: Simultaneous Aurora-A/STK15 overexpression and centrosome amplification induce chromosomal instability in tumour cells with a MIN phenotype. BMC Cancer 2007;7:212

7. Landen CN Jr, Lin YG, Immaneni A, Deavers MT, Merritt WM, Spannuth WA, Bodurka DC, Gershenson DM, Brinkley WR, Sood AK: Overexpression of the centrosomal protein Aurora-A kinase is associated with poor prognosis in epithelial ovarian cancer patients. Clin Cancer Res 2007;13:4098–4104

8. Jung CK, Jung JH, Lee KY, Kang CS, Kim M, Ko YH, Oh CS: Centrosome abnormalities in non-small cell lung cancer: Correlations with DNA aneuploidy and expression of cell cycle regulatory proteins. Pathol Res Pract 2007;203:839–847

9. Koutsami MK, Tsantoulis PK, Kouloukoussa M, Apostolopoulou K, Pateras IS, Spartinou Z, Drougou A, Evangelou K, Kittas C, Bartkova J, Bartek J, Gorgoulis VG: Centrosome abnormalities are frequently observed in non-small-cell lung cancer and are associated with aneuploidy and cyclin E overexpression. J Pathol 2006;209:512–521

10. Berrut J-P, Trefethen LN: Barycentric Lagrange interpolation. SIAM Rev 2004;46:501–517

11. Yin P-Y: Maximum entropy-based optimal threshold selection using deterministic reinforcement learning with controlled randomization. Signal Processing 2002;82:993–1006

12. Addison PS: Fractals and Chaos: An Illustrated Course. London, Institute of Physics Publishing, 1997

13. Michalak K, Kwa'Snicka H: Correlation-based feature selection strategy in classification problems. Int J Appl Math Comput Sci 2006;16:503–511

14. Terriberry TB, Joshi SC, Gerig G: Hypothesis testing with nonlinear shape models. Inform Process Med Imaging 2005; 3565:15–26

15. Kozmann G, Green LS, Lux RL: Nonparametric identification of discriminative information in body surface maps. IEEE Trans Biomed Eng 1991;38:1061–1068

16. Gustafson LM, Gleich LL, Fukasawa K, Chadwell J, Miller MA, Stambrook PJ, Gluckman JL: Centrosome hyperamplification in head and neck squamous cell carcinoma: A potential phenotypic marker of tumor aggressiveness. Laryngoscope 2000;110:1798–1801

17. Pihan GA, Wallace J, Zhou Y, Doxsey SJ: Centrosome abnormalities and chromosome instability occur together in preinvasive carcinomas. Cancer Res 2003;63:1398–1404

18. Lingle WL, Barrett SL, Negron VC, D'Assoro AB, Boeneman K, Liu W, Whitehead CM, Reynolds C, Salisbury JL: Centrosome amplification drives chromosomal instability in breast tumor development. Proc Natl Acad Sci U S A 2002;99:1978–1983

19. Sato N, Mizumoto K, Nakamura M, Maehara N, Minamishima YA, Nishio S, Nagai E, Tanaka M: Correlation between centrosome abnormalities and chromosomal instability in human pancreatic cancer cells. Cancer Genet Cytogenet 2001;126:13–19

20. D'Assoro AB, Busby R, Acu ID, Quatraro C, Reinholz MM, Farrugia DJ, Schroeder MA, Allen C, Stivala F, Galanis E, Salisbury JL: Impaired p53 function leads to centrosome amplification, acquired ERalpha phenotypic heterogeneity and distant metastases in breast cancer MCF-7 xenografts. Oncogene 2008;27:3901–3911

21. Salisbury JL, D'Assoro AB, Lingle WL: Centrosome amplification and the origin of chromosomal instability in breast cancer [review]. J Mammary Gland Biol Neoplasia 2004;9: 275–283

22. Hontz AE, Li SA, Lingle WL, Negron V, Bruzek A, Salisbury JL, Li J: Aurora A and B overexpression and centrosome amplification in early estrogen-induced tumor foci in the Syrian hamster kidney: Implications for chromosomal instability, aneuploidy, and neoplasia. Cancer Res 2007;67:2957–2963

23. Piel M, Nordberg J, Euteneuer U, Bornens M: Centrosome-dependent exit of cytokinesis in animal cells. Science 2001; 291:1550–1553

24. Shono M, Sato N, Mizumoto K, Maehara N, Nakamura M, Nagai E, Tanaka M: Stepwise progression of centrosome defects associated with local tumor growth and metastatic process of human pancreatic carcinoma cells transplanted orthotopically into nude mice. Lab Invest 2001;81:945–952

25. Hsu LC, Kapali M, Deloia JA, Gallion HH: Centrosome abnormalities in ovarian cancer. Int J Cancer 2005;113:746–751

26. Kawamura K, Moriyama M, Shiba N, Ozaki M, Tanaka T, Nojima T, Fujikawa-Yamamoto K, Ikeda R, Suzuki K: Centrosome hyperamplification and chromosomal instability in bladder cancer. Eur Urol 2003;43:505–515

27. Pihan GA, Purohit A, Wallace J, Malhotra R, Liotta L, Doxsey SJ: Centrosome defects can account for cellular and genetic changes that characterize prostate cancer progression. Cancer Res 2001;61:2212–2219

28. Guo HQ, Gao M, Ma J, Xiao T, Zhao LL, Gao Y, Pan QJ: Analysis of the cellular centrosome in fine-needle aspirations of the breast. Breast Cancer Res 2007;9:R48